IOP Conf. Series: Journal of Physics: Conf. Series **874** (2017) 012108 doi:10.1088/1742-6596/874/1/012108

Simulations and measurements of proton beam energy spectrum after energy degradation

A Gerbershagen, A Adelmann, R Dölling, D Meer, V Rizzoglio, J M Schippers
Paul Scherrer Institute, Villigen, Switzerland

alexander.gerbershagen@psi.ch

Abstract. At the proton therapy facility PROSCAN of the Paul Scherrer Institute the energy modulation of the cyclotron generated proton beam is performed via material insertion into the beam trajectory. The energy spectrum of the particles propagating forwards after such procedure has been simulated and measured. The current paper summarizes the results of these simulations and measurements and illustrates their significance for the future developments of a gantry for proton therapy at the Paul Scherrer Institute.

1. Introduction

In the cyclotron driven proton therapy facilities the energy of the proton beam is often reduced by an energy degrader [1]. At PSI it consists of six wedges composed of graphite, which are being inserted into the beam trajectory (see Figure 1). In less than 50 ms, the wedges can be moved into the beam path to a smaller or larger degree, providing all the energies in the typical range 230 – 70 MeV.

Figure 1. Depiction of degrader wedges [1].

After the degradation the beam has a momentum width, which can be higher than the momentum acceptance of the beamline and the gantries. Hence, typically an Energy Selection System (ESS) is installed downstream of the degrader. This system comprises two dipoles, a set of quadrupoles and a horizontal collimator slit (see Figure 2).

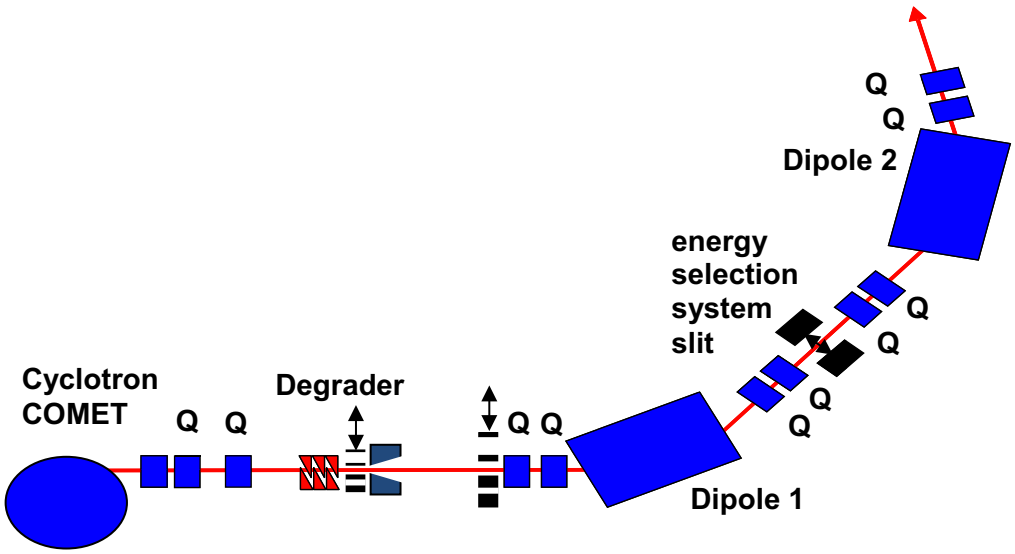

Figure 2. Layout of the first section of PROSCAN beamline with the locations of the cyclotron, the degrader, dipole magnets and energy selection system slit. Quadrupoles are labelled as "Q".

The beam optics in the ESS is arranged so that at the collimator slit location there is a focus in x-plane for a monochromatic beam (see solid red line in Figure 3). The value of horizontal beam dispersion (dotted red line in Figure 3) is high at this location (e.g. 35 mm per percent dp/p in case of PROSCAN). Hence, there is a strong correlation between the particles' horizontal position and their momentum at this location. This makes the horizontal collimator slit an effective energy selection collimator.

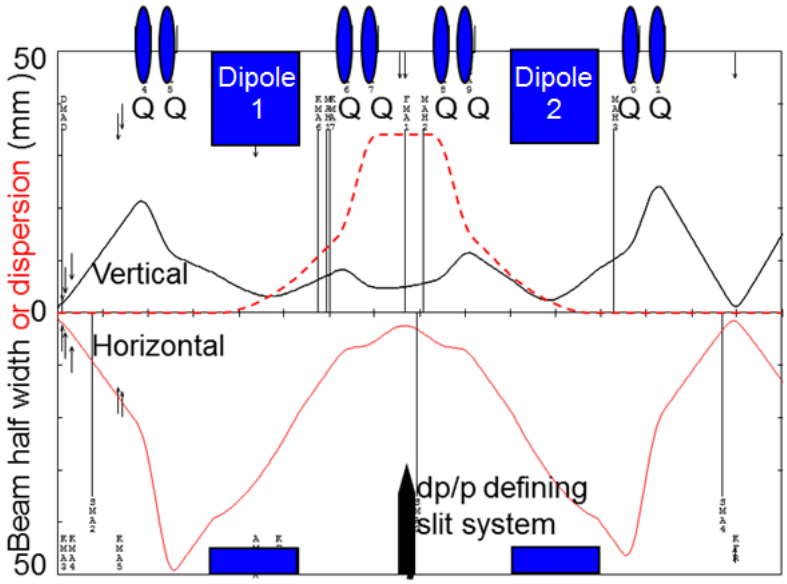

Figure 3. The TRANSPORT [2] envelope of the section presented in Figure 2. The horizontal axis is the z-position along the beam. The vertical axis above zero shows two standard deviations value of the vertical beam size (2σy). The vertical axis below zero shows the value of the horizontal beam size (2σx). The red dotted line represents the dispersion for 1% momentum offset.

Currently, a superconducting gantry including the degrader, but without ESS is being designed at PSI [3]. Such an arrangement makes the exact knowledge of the energy spectrum of a proton beam after the degradation very relevant. In the conventional ESS, as in PROSCAN, the low energy tails are absorbed by the horizontal slit. Without the ESS, as in the superconducting gantry, although the momentum acceptance of the bending section is very large, those low energies particles with strongly deviating momentum will be lost for the most part in the superconducting magnets of the final bend. Figure 4 demonstrates the trajectories of the particles with different momenta passing through the 3D field map of the proposed superconducting bend. The particle tracking has been performed with the OPAL (Object Oriented Parallel Accelerator Library) framework [4]. The five magnets of the bend have been set for the nominal beam energy of 185 MeV. The particles with the nominal energy (purple) pass well through the good field regions of all five magnets. However, particles with lower energies (orange, green and grey for 140 MeV, 90 MeV and 50 MeV, respectively) leave the good field region and will be lost at the aperture of the magnets. These particles can cause heating, which may lead to quenching of the magnet or damage the superconducting wire.

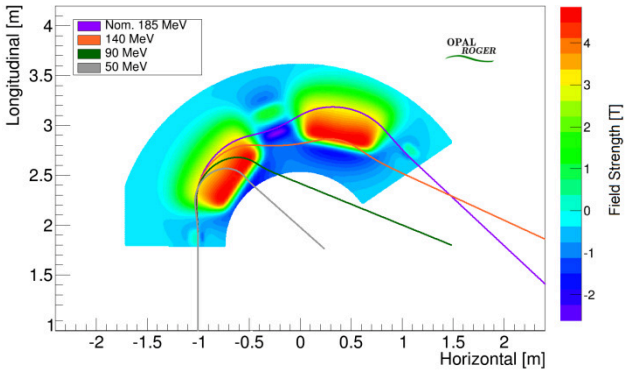

Figure 4. Trajectories of the particles tracked through a 3D field map of the proposed superconducting magnet set for 185 MeV beam.

In order to estimate how problematic this may be, simulation studies and an experiment for the determination of the beam energy spectrum have been performed and are presented in the following chapters.

2. Simulations

The energy spectrum of the proton beam interacting with the graphite degrader has been performed with the Monte Carlo code FLUKA [5]. The simulation uses $5 \cdot 10^5$ protons with an initial energy of 249.5 MeV, which corresponds to the extraction energy of the COMET cyclotron (see Figure 2). At the degrader entrance particles have a Gaussian distribution of 1.2 mm FWHM on both transversal planes and a zero divergence. The beam is assumed to be ideally monochromatic. In the FLUKA simulation, a simplified geometry of the PSI degrader of Figure 1 has been used, where the wedges have been replaced with 6 equivalent slabs of graphite with a density of 1.88 g/cm (see Figure 5). The thickness of the slabs corresponds to the thickness of the degrader wedges for the 80 MeV energy setting. Also the round collimators following the degrader, which limit the transverse emittance, are integrated in the simulation.

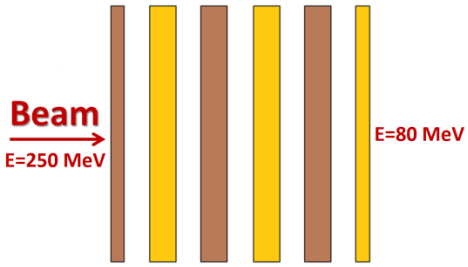

Figure 5. Schematic representation of the multi-slabs degrader geometry implemented in FLUKA.

The result of the simulated energy spectrum is shown in Figure 6, which displays the relative beam intensity as a function of energy. This distribution corresponds to a position approximately 1.5 m downstream of the degrader.

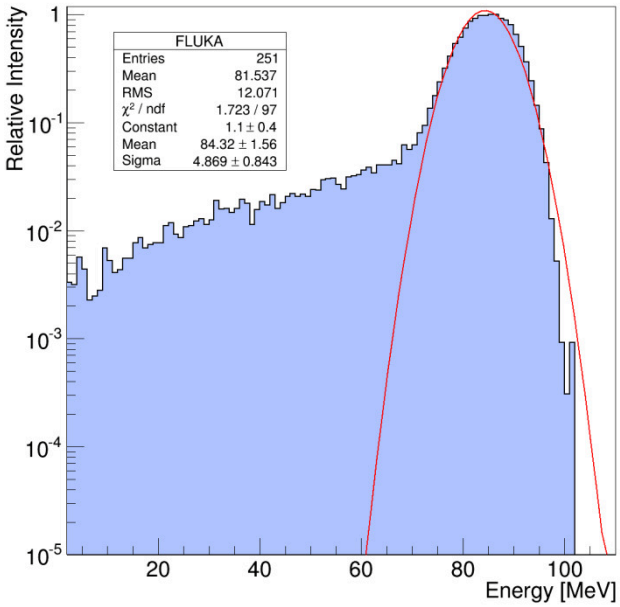

Figure 6. Simulated energy distribution after the beam propagation using the degrader parameters for the energy of 80 MeV (black curve) and Gaussian approximation of the main peak (red curve).

In Figure 6 one can observe an approximately Gaussian peak of beam intensity at approx. 80 MeV. The peak has a sharper fall-off on the high energetic side. The beam intensity above 100 MeV is negligible. However, the simulation predicts an intensity of the beam at the energies below 60 MeV at a level of approximately 0.2-2 % of the intensity maximum. The total share of the beam intensity contained in the "tail" below 70 MeV is 8.86 %. The majority of those protons underwent nuclear interactions with the degrader material.

3. Measurement

In order to measure the low energy spectrum experimentally, the degrader has been set to the energy of 80 MeV. The settings of the magnets downstream of the degrader have been adapted to transfer the beam with the lower energies between 80 MeV and 10 MeV (with the steps being 80 / 78 / 76 / 74 / 72 / 70 / 60 / 50 / 40 / 30 / 20 / 10 MeV). For this, the nominal magnet settings for the energy of 80 MeV used for PSI Gantry 3 has been scaled down with the momentum of the beam. The beam profile in front of the ESS slit location has been recorded for each step in the energy using a strip profile monitor.

Due to the high correlation of the horizontal position of the particles and their energy at the location of ESS, the beam intensity measured in the center of the strip monitor corresponds to the beam intensity for a given energy.

The projection of the horizontal profile directly in front of the ESS slit has been measured by a relatively thick ionization profile monitor [6] using an automated procedure [7]. The beam currents to the central 14 strips are derived from the signal currents taking into account the energy dependent amplification and the energy loss of the protons in the chamber foils (Figure 7). At 10 MeV, the beam energy was too low to reach the active volume of the monitor, resulting in a signal below the amplifier threshold of a few pA.

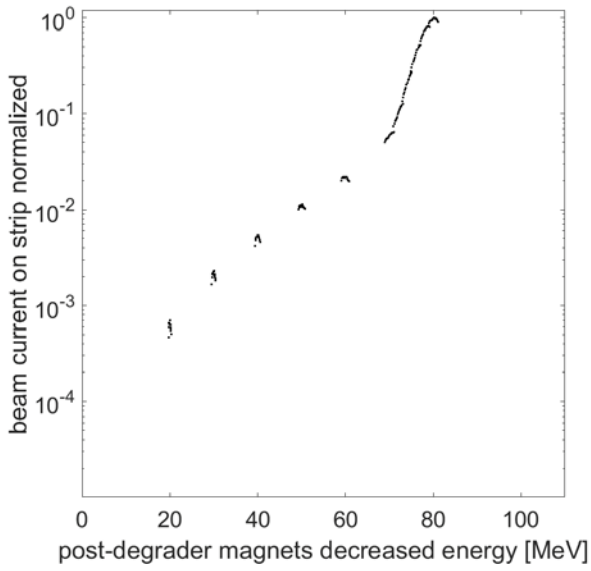

Figure 7. Relative beam intensity as a function of beamline setting energy, measured at the ESS slit location.

In Figure 7 one can recognize the Gaussian peak with a maximum at 80 MeV. At the energies below 70 MeV there is a tail of low energy particles. The transition of Gaussian peak to exponential tail appears at approximately 5 % of the peak intensity. This compares well to the 6 % of the simulation. Also the transition energy of 70 MeV from the Gaussian peak to the tail compares well to the simulation prediction. The general shape of the tail corresponds well to the simulation result displayed in Figure 6. This suggests that the particles populating it correspond to the particles involved into the nuclear interactions in the degrader, as predicted in the simulation.

There is an observed fall-off of the individual profiles to the sides for the energies below 70 MeV. One possible explanation for it is that the particles with a momentum strongly deviating from the beamline setting are lost before the beam arrives at the ESS slit, since in there are two more collimators limiting the beam size horizontally after the first dipole introduces the dispersion. This may also indicate that the measured intensity is too low at low energies.

At lower energies the relative intensity in the simulation results becomes increasingly larger than the measured intensity, e.g. at 20 MeV the difference is about by a factor of 10. We expect that for these low energies the signal of the monitors is too low. Also, the measurement relates to a position, which is approximately 6 m downstream of the position considered in the simulation. Two additional collimators are in between. It is plausible that the transmission over this line is lower for the low energy protons which start with a broader angular distribution.

4. Conclusions and outlook

The results of the FLUKA simulation for the spectrum of the beam after degradation are consistent with the measurement results in the significant, high energy part of the spectrum. This indicates that the effects providing the largest contribution to the beam energy loss, incl. multiple nuclear scattering and the inelastic scattering, are correctly implemented in FLUKA and that FLUKA simulations can be used as a reliable tool for the further studies.

These studies will include the OPAL simulation of the beam with the described spectrum being propagated through the superconducting magnet bend described above (Figure 4). The goal of the simulations is to determine the locations along the bend at which the low energy particles reach the magnet aperture, and hence get lost. The simulations will give a comprehension of what the total power deposited at each bend location will be and how the particles will interact with the vacuum pipe or magnet material. It is expected that the largest share of losses will occur on the inner aperture of the first half of the bend. Also, some protons with a very low energy will take a spiral trajectory transversely to the bending plane and will be lost on the magnet aperture in the non-bending direction at the entrance of the first superconducting dipole.

There are following possible consequences of the beam losses in the superconducting magnet:

a) Long term damage of the superconducting material.
b) Warming up of some locations in the SC magnet and generation of so-called hot spots in the superconductor. The hot spots can increase the probability of quenches. These are very undesirable in the magnet, which must have a very high reliability (and up-time) for the purpose of medical treatments. If the simulations demonstrate that the warming up of the superconducting coil is a problem, the cooling and quench prevention concepts need to be revised.
c) Activation of the gantry material and the area around the patient. Also, the neutron production from the scattered protons must be calculated and the neutron dose the patient will receive due to the lost low energy tail of the proton beam must be estimated.

We are designing a material inlayer at the inner aperture of the bend (in the bending plane), which will absorb the majority of the particles. The material should be selected so that a proton beam scattered on it causes a relatively small activation and a relatively low neutron production.

References

[1] Reist H *et al.* 2003 Concept for Handling and Service of the Proscan Degrader Unit *PSI - Scientific and Technical Report* Volume VI p. 109
[2] Rohrer U PSI Graphic Transport Framework. based on a CERN-SLAC-FERMILAB version by K.L. Brown et al.
[3] Gerbershagen A *et al.* 2016 A novel beam optics concept in a particle therapy gantry utilizing the advantages of superconducting magnets *Zeitschrift für Medizinische Physik* vol. **26** no. 3 p. 224–237

[4] Adelmann A, Gsell A, Metzger-Kraus C, Ineichen Y, Russel S, Wang C, Yang J, Sheehy S, Rogers C and Winklehner D 2008 - 2017 The OPAL (Object Oriented Parallel Accelerator Library) Framework *Technical Report* PSI-PR-08-02
[5] Ferrari A, Sala P, Fasso A and Ranft J 2005 *FLUKA: a multi-particle transport code* CERN-2005-10
[6] Dölling R *et al.* 2007 Beam Diagnostics for the Proton Therapy Facility PROSCAN *Proc. Acc. App.* pp. 152-159
[7] Dölling R 2016 Automated Documentation of Tunes in the Beam Lines of the COMET Cyclotron *Cyclotrons Conference Procedings* Zürich Switzerland THP17